Hindawi
Advances in Civil Engineering
Volume 2021, Article ID 8481571, 10 pages
https://doi.org/10.1155/2021/8481571

Research Article

Study on the Process and Characteristics of Clogging for Ceramic Permeable Brick

Zizeng Lin,[1] **Hai Yang**,[2] **and Huiming Chen**[1]

[1]*College of Civil Engineering, Nanjing Forestry University, Nanjing, China*
[2]*Sichuan Road & Bridge (Group) Corporation LTD, Chengdu, China*

Correspondence should be addressed to Zizeng Lin; linzizeng@njfu.edu.cn

Received 3 December 2019; Revised 2 December 2020; Accepted 30 December 2020; Published 8 January 2021

Academic Editor: Hui Yao

A ceramic permeable brick was selected for study in a device that was designed to fully investigate the process and characteristics of clogging in permeable bricks. In order to evaluate the permeability influenced by clogging, a simulated rainfall was filtered through the permeable brick placed in an innovative device. The macroscopic and microscopic changes in the brick and the filtrate were all measured to fully investigate the causes and process of clogging. Then, the mechanism of clogging in the permeable brick pores was further discussed. The results showed that the clogging risk of permeable brick was extremely high, and it can result in a complete clogging in only 5–10 years under the experimental conditions. The permeability coefficient and porosity both decreased exponentially with the increase in filtrate, which was attributed to the clogging of the internal pore structure due to particle interception. The chord size distribution results stressed that the blockage mainly occurred in the upper layer pores in the range of 0.5–1.5 mm, which is relatively sensitive to clogging due to the particle size distribution in rain water. The particle size distribution of the influent and effluent indicated that the clogging process could completely remove particles larger than 88 μm but showed variable removal efficiency for particles with sizes of 20–88 μm. This research offers new insight into the clogging of permeable bricks and provides theoretical guidance for restoring the brick permeability.

1. Introduction

In recent years, permeable pavements have become one of the most frequently used low impact development (LID) techniques [1]. This infiltration-based technology comprises structural layers with relatively high porosity to allow rainwater to pass through its surface and underlying layers. Permeable pavements are composed of a permeable pavement surface and aggregate subbases and sometimes include geotextiles and underdrains. Rainwater eventually permeates into the natural soil or discharges into a drainage system [2].

The permeable brick paving system (PPS) played a significant role in the hydrological effect and the reduction in rainwater pollution. The hydrological effect of the PPS contributed to a reduction in the volume of rainwater runoff and recharging of the ground water [3–6], indicating the sufficient permeability of the permeable brick layer in a PPS. In addition to reducing runoff, delaying peak flow, and increasing the infiltration rate, permeable brick also exhibits favorable decontamination potential, especially for the removal of total suspend solids (TSS). Li et al. found that the average removal efficiency of TSS was approximately 90.0% for six commonly used surface materials (porous asphalt, porous concrete, cement brick, ceramic brick, sand base brick, and shale brick) because of physical interception [7]. Due to the high removal capacity of TSS in urban runoff, physical blockage is inevitable, which is why clogging has been defined as the accumulation of silt within the brick due to sedimentation [8, 9]. With the increase in the retention of solid particles, the permeable bricks are gradually blocked, and their effective service duration basically terminates [10–12]. Then, a suction sweeping or high-pressure water jet can be used to restore the permeability [13, 14].

The most common factor causing brick failure was clogging, and this brick clogging was affected by the particles

in rainwater. Pratt et al. found that physical clogging could result from the accumulation of fine particles in the void spaces of porous pavements [15], while Balades et al. determined that the particle size also played a key role in the clogging process [16]. Other scholars further revealed that size and fraction were the most important factors influencing physical clogging. For example, Kayhanian et al. stated that particles with sizes less than 38 μm, which accounted for more than 95% of the particles, were one of the main factors that influenced the permeability [17]. Siriwardene et al. demonstrated that physical clogging was mainly caused by the migration of sediment particles less than 6 μm in diameter [18]. However, it was not comprehensive to evaluate brick clogging only by particles in rainwater. In fact, the size of the clogging particles relative to the pore size in permeable brick is also an important influencing factor [19]. Therefore, the pore structure distribution inside the brick is also extremely important.

Currently, a commonly used tool for assessing brick clogging is through the measurement of the permeability coefficient because this parameter is directly related to the content of brick pores [20]. When the pores in the permeable brick were clogged to some extent, the pavement permeability decreased, and its permeability coefficient drastically reduced. An earlier study reported that infiltration capacities of the permeable brick reduced to 19 and 7–12 mm/min from 290 and 470 mm/min, respectively, without any maintenance for nearly two years [21]. However, these data are not enough to understand the essentially microscopic process through macroscopic parameters such as permeability coefficient, and it is likely to gain more insight if the microscopic processes are inspected directly. Therefore, more attention should be focused on parameters such as the particle size distribution of the runoff sediment and the pore structure distribution inside the brick, which are characterized from the microscopic perspective.

Ceramic permeable brick is commonly used in Chinese market because of its compact structure and good hydrological performance. In this study, ceramic permeable brick was selected and used to investigate the clogging process. A simulated rainfall was filtered through the permeable brick placed in the device to measure the macroscopic parameters such as permeability coefficient, removal rate of TSS, and total interception quantity of TSS. Moreover, the microscopic parameters, such as the pore structure distribution inside the brick and the particle size distribution of the influent and effluent, were all detected. Then, the mechanism of clogging in the permeable brick pores was further discussed. This research used a self-designed device, which was combined with the macroscopic and microscopic changes in the brick and filtrate, to investigate the causes and clogging process of a permeable brick, and it can offer a new insight into the clogging of permeable bricks.

2. Materials and Methods

2.1. Simulate Rainwater. The kaolin was grounded and screened by standard sieve to remove particles with diameter larger than 0.106 mm, and then the simulated rainwater of 1000 mg/L was configured by using kaolin power with pure water, which was basically the same as the TSS concentration in the initial rainwater of Nanjing. The laser particle size analysis was carried out to obtain its particle size distribution, which is displayed in Figure 1.

Results presented in Figure 1 showed that the particle size distribution range was mainly 0.45–20 μm, the particles smaller than 74 μm accounted for about 98%, and the maximum particle size was 104.7 μm. Particle size distribution was basically consistent with the existence form of particulate matter in rainwater. For instance, Duncan found that particles smaller than 85 μm accounted for about 90% in rainwater [22]. Besides, Zuo investigated the particle size of rainwater runoff in Nanjing and found that the particles in the range of 0.45–20 μm were the most, accounting for about 37.5% of the total particles [23].

2.2. Permeable Brick. Using waste ceramics as the main raw material, ceramic permeable bricks are manufactured by sintered at 1200°C, which were mainly used in the construction of permeable pavements in city parks, squares, parking lots, and residential areas. The ceramic permeable bricks measured 20 cm × 20 cm × 5.5 cm and were purchased from Youbang Building Materials Co., Ltd. As displayed in Figure 2, similar to all permeable bricks in the Chinese market at present, the ceramic brick can be divided into two layers in a common configuration. The upper layer has a thickness of approximately 1.0 cm with a relatively smaller diameter of the particle, and the lower layer is approximately 4.5 cm.

The chord size distribution and porosity of the brick were obtained by measuring the pore structure. The chord size distribution of the brick is shown in Figure 3. Results are presented in Figure 3, and the upper layer cross-section of the ceramic permeable brick had a smaller proportion of pores in the 0.5–4.0 mm size specification than in the lower layer, while the two layers had porosities of 24.82% and 58.66%, respectively. Clearly, the presence of a larger pore size increased the porosity of the lower layer and the distribution of the pores. Small pores, located on the top, and large pores, located on the bottom, objectively make the surface layer function as a sieve, and the surface layer may play a more critical role in the purification process.

The main properties are shown in Table 1, and the chemical composition is shown in Table 2. The main properties of the brick, such as splitting tensile strength, permeability coefficient, frost resistance, slip resistance, and porosity, all met the requirements of the Chinese National Standard (Permeable paving bricks and permeable paving flags) (GB/T 25993–2010). The permeability coefficient of permeable brick was 3.1×10^{-2} cm/s, which was larger than the standard permeability coefficient at 2.0×10^{-2} cm/s.

2.3. Apparatus. The device was self-designed according to the Chinese national standard of permeable paving bricks and permeable paving flags (GB/T 25993–2010) (Figure 4). The permeability coefficient was measured using the

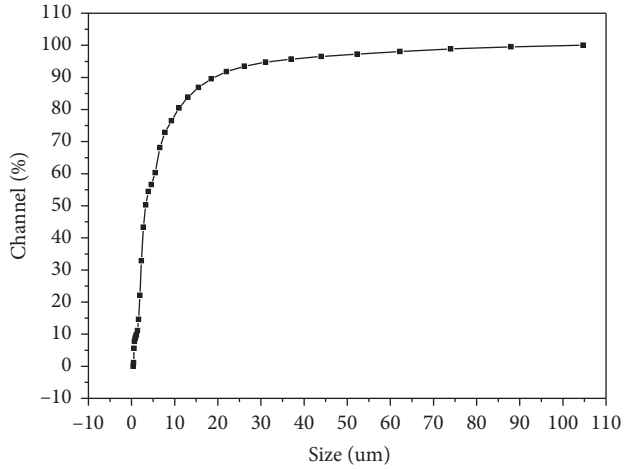

Figure 1: Particle size distribution of simulate rainwater.

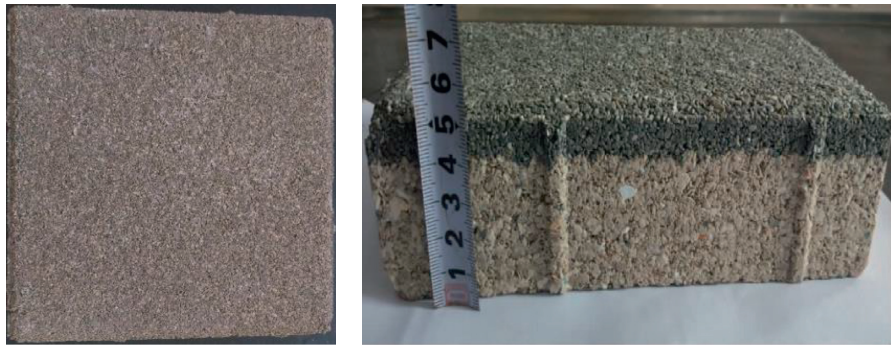

(a) (b)

Figure 2: Ceramic permeable brick. (a) Surface. (b) Section.

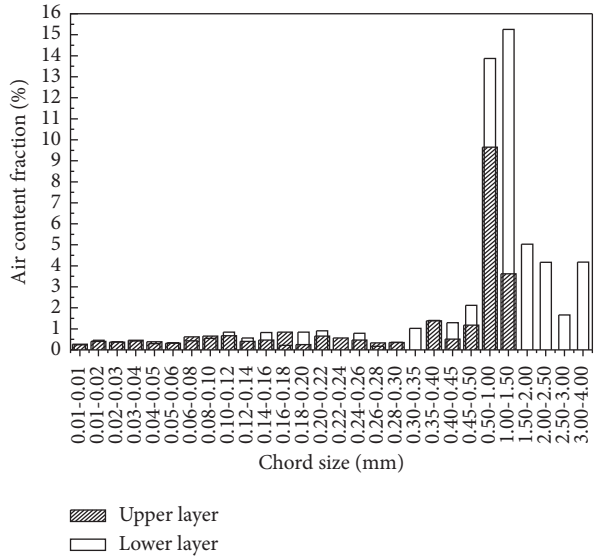

Figure 3: Chord size distribution of the brick.

Table 1: The main properties of ceramic permeable brick.

Index	Splitting tensile strength (MPa)		Permeability coefficient (cm/s)	Frost resistance (%)	BNP	Porosity (%)
GB/T25993-2010	Average value ≥ 4.5	Minimum value ≥ 3.4	$\geq 2.0 \times 10^{-2}$	Strength loss rate ≤ 20	≥65	≥15
Ceramic brick	5.3	4.7	3.1×10^{-2}	4	89	24.82

BPN, British Pendulum Number.

Table 2: Chemical composition of ceramic permeable brick.

Composition	SiO_2	Al_2O_3	CaO	K_2O	Fe_2O_3	MgO	Na_2O	Else
Ceramic brick	69.32	17.50	2.58	2.23	1.42	1.32	3.98	1.65

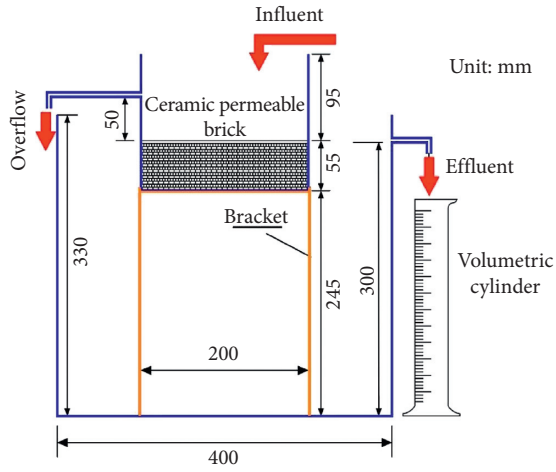

Figure 4: The experimental apparatus.

constant head method, which followed Darcy's law, and can be expressed by the following formula:

$$K = \frac{VL}{AHT}, \quad (1)$$

where K is the permeability coefficient, V is the water volume, L is the height of brick, 5.5 cm, A is the cross-sectional surface area of brick, 400 cm^2, H is the water level difference from the upper surface of the brick to the bottom of the overflow pipe, 5.0 cm, and T is the duration of the experiment.

2.4. Test Methods. The main properties of the brick were determined according to the Chinese National Standard (permeable paving bricks and permeable paving flags) (GB/T 25993–2010), the compositions were measured by using ARL9800XP (Thermo Fisher, USA), and the chord size distribution and porosity of the brick were measured using an air-void analyzer (Rapid air 457, Germany) according to the linear transverse winding test of the standard test method for microscopical determination of parameters of the air-void system in hardened concrete (ASTM C457). The sample was tested after sanding, polishing, and color enhancement, and the stomatal pore of the sample appeared white, while the rest appeared black. According to the Chinese National Standard Methods (SEPA of China 2002), TSS were determined by gravimetric method (GB 11901–89). According to the Chinese National Standard of particle size analysis-laser diffraction methods (GB/T 19077–2016), the sample was poured into liquid paraffin and shaken for 10 min in an ultrasonic environment. The particle size distribution of the sediment in the influent and effluent was measured using a laser particle size analyzer (Mastersizer 3000, England).

In the test, the removal rate (R_r) and cumulative interception quantity (CIQ) were as equations (2) and (3):

$$R_r = \frac{1000 - SS_e}{1000} \times 100\%, \quad (2)$$

$$CIQ = \frac{\sum 1000\,\text{mg}}{L \times V \times Rr}, \quad (3)$$

where 1000 mg/L is the concentration of the influent, SS_e is the measured concentration of the effluent, and V is the filtrate volume.

3. Results and Discussion

3.1. Permeability Coefficient of Permeable Brick. The relationship between permeability coefficient and filtration volume is shown in Figure 5. As the filtration volume increased, the permeability coefficient values greatly decreased, and the slope of the permeability coefficient curve at

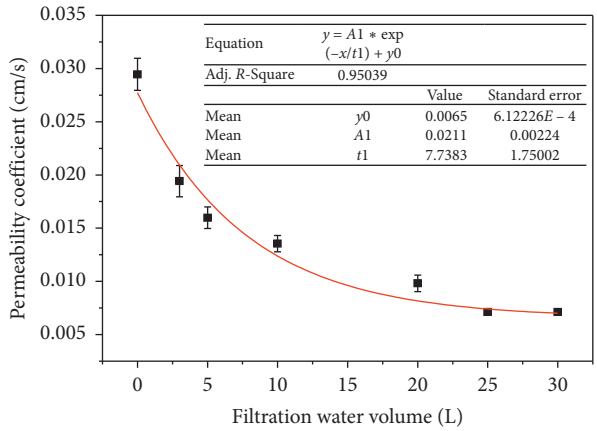

Figure 5: Changes in the permeability coefficient with filtration volume.

the initial stage was significantly higher than that at the later stage. During the initial infiltration process, the interior of the permeable brick was relatively clean, and large particles quickly precipitated in the voids inside the brick and blocked the outflow pores of the effluent, which led to a rapid decrease in the permeability coefficient [24, 25]. With the increase of the filtration volume, small particles were either tightly adhering to the pores or captured and bonded by the large particles, which gradually blocked the pores of permeable brick. Then, the connectivity of holes was getting worse, and correspondingly, the permeability coefficient gradually decreased because the connected porosity was the most important factor to influence the permeability [26, 27], and finally it turned to be stable until the hydraulic performance was basically lost [28].

The result was highly consistent with the conclusion of other researchers; that is, the permeability coefficient decreased exponentially with the increase in filtration volume [29, 30]. When the filtration volume accumulated to 20 L, the permeability coefficient decreased from the initial 0.030 cm/s to 0.010 cm/s with a decrease of 67%. According to the Chinese National Standard that specifies that the permeability coefficient must be larger than 0.010 cm/s, the ceramic permeable brick had lost its function when the infiltration volume accumulated to 20 L, with the average annual precipitation of Nanjing City calculated as 1110 mm and with the Sponge City Construction requirement that 70% of the precipitation be absorbed in situ, which meant that 770 mm rainfall passed through permeable bricks. Combined with the formula of rainfall intensity and the distribution of the rainfall frequency in Nanjing, it was found that it only took about half a year for such rainfall amount penetrating through the brick. Then, the effective service duration of permeable brick was only approximately 0.5 years under the TSS concentration condition of 1000 mg/L and with no maintenance of the permeable brick. If the filtration volume was calculated according to the first 15 min for a rainfall event to 120 min, the effective service life was only 5–10 years, which is shorter than the calculated results for other permeable pavements. For instance, a long-term research found the two pavements being significantly clogged after being in use for 18 and 24 years [21], while Pratt et al. predicted the effective service life of permeable pavements to be 15–20 years using simulation experiments [31]. The experimental result of brick clogging was shorter than that of permeable pavements. In other words, the clogging risk of permeable brick was very high.

The result presented here was highly consistent with the observed clogging behavior of pervious concrete [32, 33], which revealed that the blockage of pore channels, porosity reduction, and/or tortuosity increase were also the main cause of the clogging. Therefore, it is necessary to study the pore changes in the clogging process.

3.2. Porosity and Chord Size Distribution. There were many irregular voids and pores inside the permeable brick to improve the permeability effect. Porosity and chord size distribution were two important indicators characterizing the brick clogging, which represented the number of total pores and the form of pore structure, respectively. Because the pores are not strictly circular, thus, the chord size of the longitudinal section was used to represent the size of the irregular pores, which could reflect the 3D pore parameters such as tortuosity, constrictivity, and connectivity indirectly, For instance, the smaller the size of the hole, perhaps, the better the connectivity of the 3D pore hole. In addition, the chord length frequency was used to represent the number of pores. Porosity would decrease when the brick is clogged, and the chord size distribution was bound to change. Therefore, the clogging process could be revealed by studying the changes in these two indicators.

The porosity change in the upper layer and lower layer with different filtration volumes is presented in Figure 6. The porosity of the lower layer was stabilized, with a value of approximately 60% in the clogging process, while the fraction of the upper layer significantly decreased (Figure 6). This result showed that the blockage mainly occurred in the upper surface of the brick and had little relationship with the lower layer. Previous studies found that clogging was most likely to occur near the upper 2.5 cm or 1.25–2 cm of the permeable brick [14, 34], and the clogged layer acted as a sieve that reduced the sediments that tended to accumulate in the pores at the bottom of the brick. However, in our study, the clogging of the upper layer was more likely to be caused by the different structures of permeable brick, and the structural configuration of ceramic brick was objectively beneficial to the interception of particles. The declining trend in porosity also obeyed the law of exponential change and was highly consistent with the permeability coefficient. The similarity might be because the internal pore structure was affected by the particle interception, which included surface filtration, inner blocking, and attachment [35], and it further affected the internal porosity and apparent permeability coefficient. Therefore, the chord size distribution needs to be further discussed.

The chord size distribution for ceramic permeable brick with different filtration volumes is shown in Figure 7. Results presented in Figure 7 showed that the large chord with a size of 0.5–1.5 mm was most influenced by the blockage process,

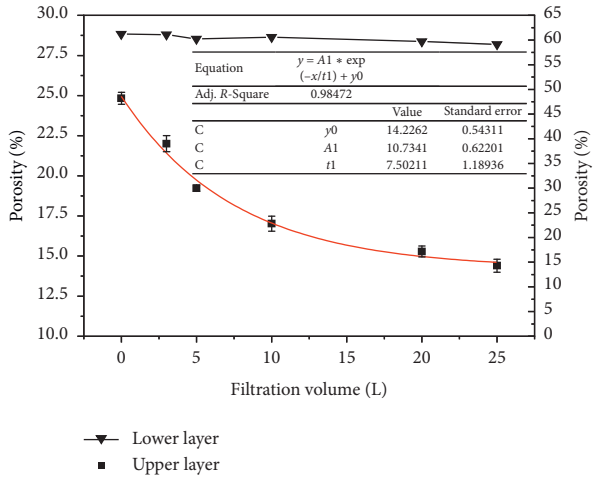

Figure 6: The porosity change of the upper layer and lower layer with filtration water.

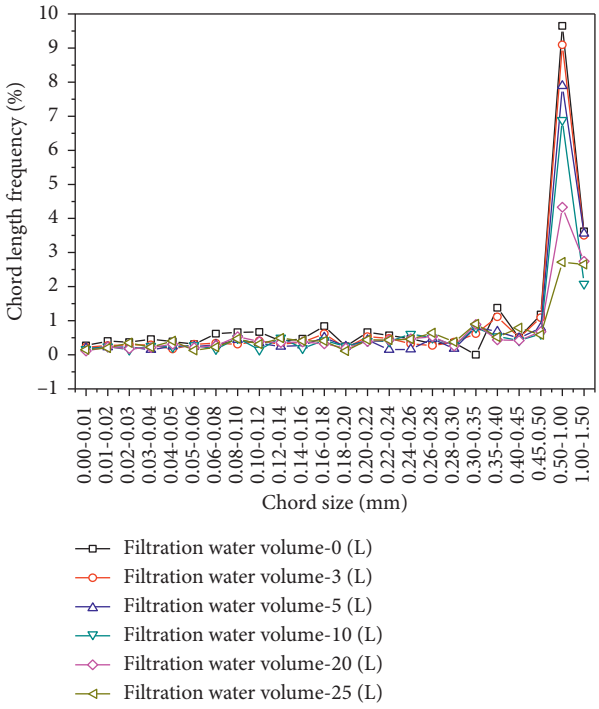

Figure 7: Chord size distribution with the different filtration volumes.

and other smaller chords were minimally affected. The chord length frequency of brick decreased from 10% to 2.5% with a decrease of 75%, while the volume of water increased from 0 to 25 L. The main clogging range might be related to the particle size distribution in the rainwater. According to the research of Deo et al. [36], when the pore size was about 7 times of the maximum particle size, the clogging was most likely to occur. In this experiment, the maximum particle size range was 74–104.7 μm, and 7-fold clogging size was 0.52–0.73 mm, which was just within the range of 0.5–1.5 mm. At this time, particulates were easily congested or squeezed into this pore size range, which made it difficult to continue to move downwards under the action of (in spite of) water and air flow. Furthermore, the particulates evolved into new skeletal particles, resulting in fewer pore channels and lower pore ratios [37], and interlocking of the pores with clogging particles [38]. Another reason why the large pores were easily blocked might be that the speed of rainwater passing through the large pores was slower [39]. The particles were more likely to aggregate because the hydraulic shearing force of the large pores was smaller and conducive to settling. It could be further speculated that the clogging of the big pores was the reason for the exponential decline of permeability coefficient and porosity. The pore size determined whether clogging particles could pass through the pores or not [38]; obviously, the big hole had a more direct influence in this aspect.

In summary, the blockage of the upper layer was the main reason for the clogging of the permeable brick, and the pore size distribution within the range of 0.5–1.5 mm was relatively sensitive to particles in the simulated clogging solution, which further validated the 7-fold clogging theory.

3.3. Removal Rate and Cumulative Interception Quantity. The relationship between the filtration volume and the removal rate and cumulative interception is presented in Figure 8. As the amount of filtration volume increased, the removal rate decreased, while the total amount of interception inside the permeable brick increased. With the brick heavily clogged, the diameter of internal pore decreased; meanwhile, the shearing force of water flow increased under water pressure, so that TSS was not easy to be physically intercepted by brick, which led to the reduction of removal rate [40]. Moreover, some of the intercepted TSS were also released under the runoff infiltration, resulting in a high effluent concentration and a low removal rate [25, 39]. The initial TSS removal rate was approximately 70% for the original ceramic permeable brick, and the removal rate was approximately 39.05% when the filtered water volume was 20 L. At this time, the permeability coefficient was 0.099 cm/s, which was just lower than the national standard of 0.1 cm/s, with the cumulative interception amount being approximately 7779.8 mg/cm^2. When the filtered water volume was 35 L with a removal rate of approximately 10.3%, the interception and decontamination performance of the TSS in the permeable brick were basically lost, which meant that the pores inside the permeable brick were almost saturated. At this time, the cumulative interception amount was approximately 11000 mg/cm^2.

3.4. Particle Size Distribution of Influent and Effluent. Changes in particle size distribution in the influent and effluent with different volume of filtration water are presented in Figure 9. Results presented in Figure 9 showed that the maximum particle diameter of the influent was 104.7 μm and that of the effluent was only 66.23–88 μm, indicating that the particles with diameters of 88–104.7 μm were almost all removed. It may be because some large particles have their own characteristics, and once deposited in the pores of permeable bricks, it is difficult for them to move down with

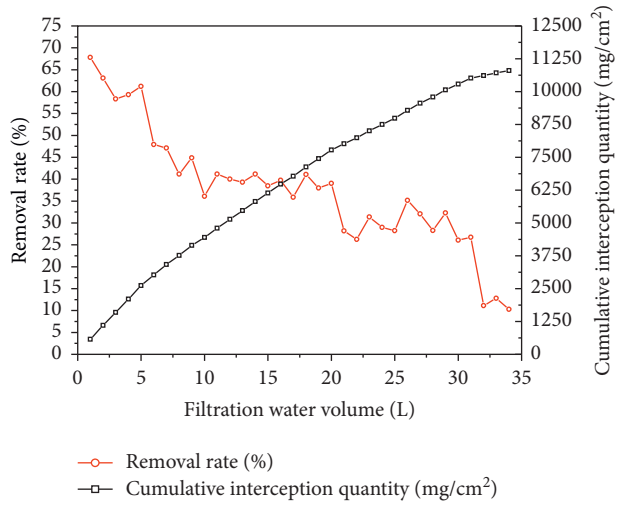

Figure 8: The relationship between the filtration volume and the removal rate and cumulative interception quantity.

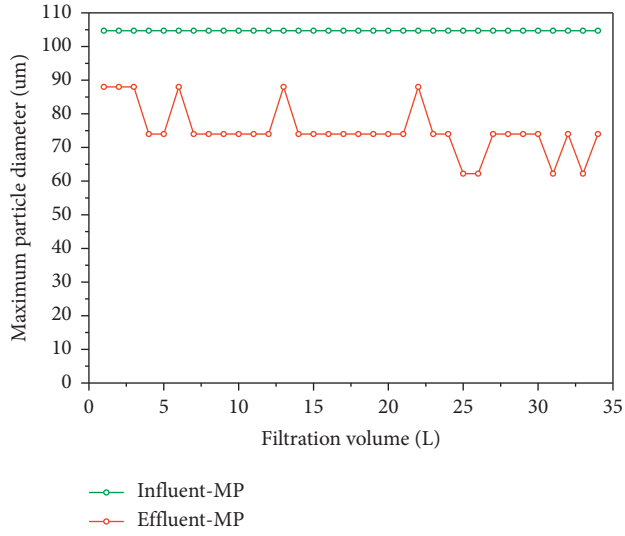

Figure 9: Changes of the maximum particle diameter of influent and effluent with different filtration volume.

the water flow [19, 41]. The maximum particle diameter of the effluent remained stable at 66.23–88 μm, showing that the effective minimum filtration diameter of the brick was approximately 88 μm. Therefore, particles larger than 88 μm were almost completely removed.

The particle size distributions of the water samples with different removal rates are shown in Figure 10. The particles larger than 88 μm were completely removed from the effluent with a removal rate of 58.34% (Figure 10(b)) compared with the raw water (Figure 10(a)), and the particles between 74 and 88 μm were further removed with a removal rate of 41.18% (Figure 10(c)) compared with the effluent with a removal rate of 58.34% (Figure 10(b)). The main reason was that the large particles were trapped by the upper layer of the permeable brick as the amount of filtered water increased, and the small particles continuously migrated downward, resulting in a decrease in the overall pore diameter, which further reduced the particle size of the retained particles. The particle size distribution with a removal rate of 26.75% (Figure 10(d)) had little change compared to the effluent with a removal rate of 41.18% (Figure 10(c)), suggesting that the later interception of smaller particles might be dominated by the average removal. From the total passing rate, the particle size of the filtered water was generally below 20 μm, indicating that the effective maximum filtration diameter of permeable brick might be approximately 20 μm. Therefore, particles smaller than 20 μm were hardly removed. The experimental results further proved that fine particles had a great influence on the clogging phenomenon [42]. Overall, the particles larger than 88 μm were almost removed completely, the particles within 20–88 μm were removed in variable amounts, and almost all the particles smaller than 20 μm passed through the brick during the clogging process. Moreover, it is necessary to note that the result is relevant to the sample tested and the influent used in this study.

In general, the clogging risk of ceramic permeable brick is relatively high. Therefore, in field applications, it should be

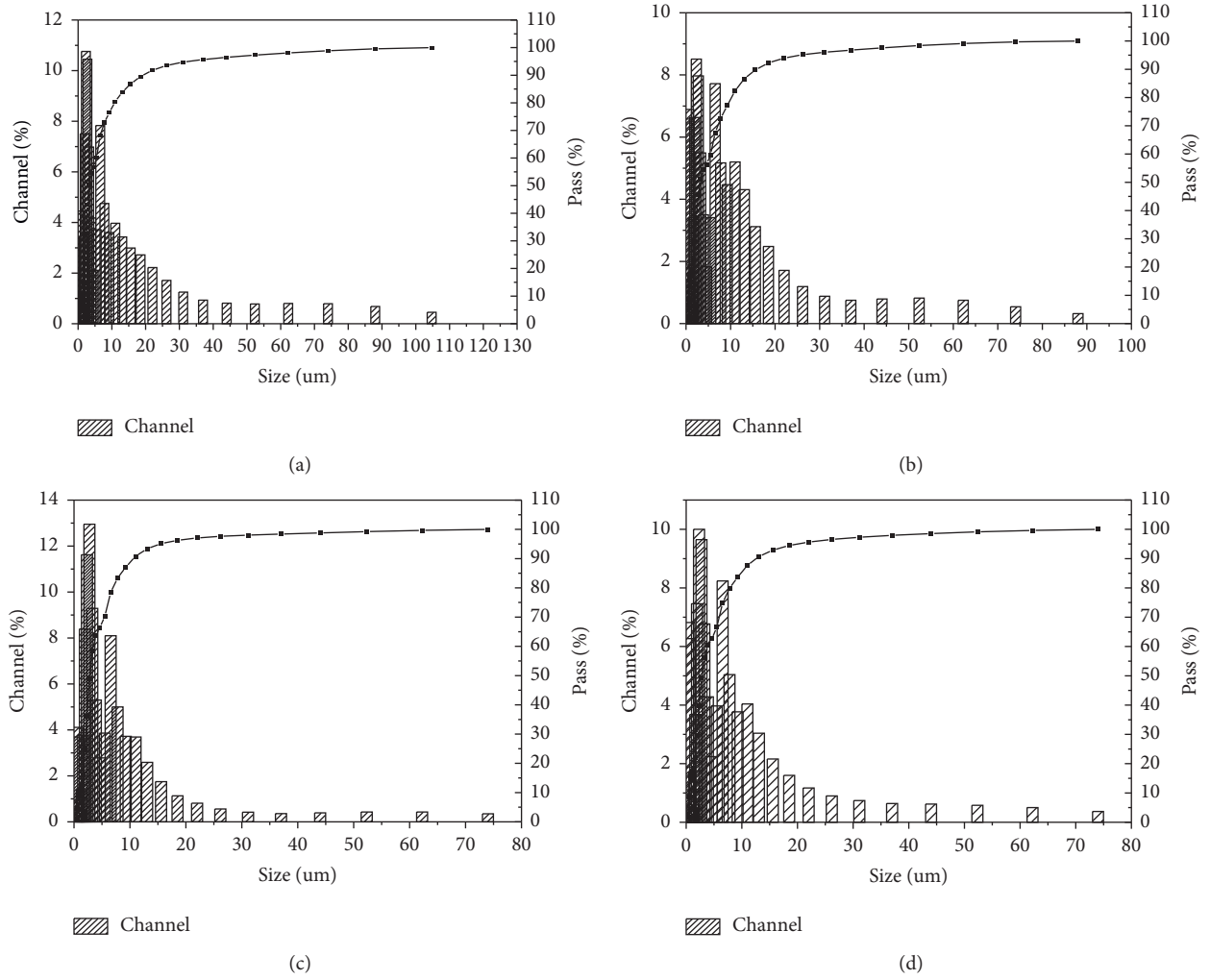

Figure 10: Particle size distribution of the water samples with different removal rates. (a) Raw water. (b) Effluent with a removal rate of 58.34%. (c) Effluent with a removal rate of 41.48%. (d) Effluent with a removal rate of 26.75%.

used in the places such as city parks, squares, parking lots, and residential areas, where fine particles are relatively few, and it is not suitable for use on roads with heavy traffic load. In the future research, the study of the clogging mechanism should be combined with the study on the effect of cleaning and restoration to find better recovery measures.

4. Conclusions

(1) The permeability coefficient decreased exponentially with increasing time, which was highly consistent with the change in porosity in the upper layer. The reason for the similarity might be that the clogging of the internal pore structure affected the pore size distribution and further affected the permeability coefficient of the brick. The effective period of permeable bricks, based on calculations of the actual situation in Nanjing, was only 5–10 years, so the clogging risk of permeable brick is extremely high.

(2) The blockage mainly occurred on the upper surface of the brick and had little relationship with the lower layer. The larger pores within 0.5–1.5 mm were sensitive and easily influenced by the blockage process due to the particle size distribution in rain water.

(3) With the increasing amount of filtration volume, the removal rate decreased, and the total amount of interception increased. The removal rate of TSS decreased nearly by half with the loss of the filtration function, while the cumulative interception amounted to nearly 7779.8 mg/cm^2.

(4) The particle size distribution of the influent and effluent showed that the particles larger than 88 μm were almost completely removed, the particles with sizes of 20–88 μm were removed in variable amounts, and the particles smaller than 20 μm were almost completely passed through the brick during the clogging process.

Data Availability

The data used to support the findings of this study are available from the corresponding author upon request.

Conflicts of Interest

The authors declare that they have no conflicts of interest.

Acknowledgments

This study was supported by the National Natural Science Foundation of China (No. 51608272), the Science and Technology Project of Jiangsu provincial Construction System (No. 2018ZD203), and the Student's Innovative Projects of Nanjing Forestry University (2018NFUSPITP769) for financial support.

References

[1] Z. -G. Niu, Z. -W. Lv, Y. Zhang, and Z. -Z. Cui, "Stormwater infiltration and surface runoff pollution reduction performance of permeable pavement layers," *Environmental Science and Pollution Research*, vol. 23, no. 3, pp. 2576–2587, 2016.

[2] L. Chu and T. F. Fwa, "Evaluation of surface infiltration performance of permeable pavements," *Journal of Environmental Management*, vol. 238, pp. 136–143, 2019.

[3] R. M. Roseen, T. P. Ballestero, J. J. Houle et al., "Seasonal performance variations for storm-water management systems in cold climate conditions," *Journal of Environmental Engineering*, vol. 135, no. 3, pp. 128–137, 2009.

[4] C. J. Pratt, A. P. Newman, and P. C. Bond, "Mineral oil biodegradation within a permeable pavement: long term observations," *Water Science and Technology*, vol. 39, no. 2, pp. 103–109, 1999.

[5] B. O. Brattebo and D. B. Booth, "Long-term stormwater quantity and quality performance of permeable pavement systems," *Water Research*, vol. 37, no. 18, pp. 4369–4376, 2003.

[6] C. T. Andersen, I. D. L. Foster, and C. J. Pratt, "The role of urban surfaces (permeable pavements) in regulating drainage and evaporation: development of a laboratory simulation experiment," *Hydrological Processes*, vol. 13, no. 4, pp. 597–609, 1999.

[7] H. Li, Z. Li, X. Zhang et al., "The effect of different surface materials on runoff quality in permeable pavement systems," *Environmental Science and Pollution Research*, vol. 24, no. 26, pp. 21103–21110, 2017.

[8] C. Dierkes, L. Kuhlmann, K. Jaya, and A. George, "Pollution retention capability and maintenance of permeable pavements,," in *Proceedings of the 9th International Conference on Urban Drainage (9ICUD)*, Portland, OR, USA, September 2002.

[9] N. González-Angullo, D. Castro, J. Rodríguez-Hernández, and J. W. Davies, "Runoff infiltration to permeable paving in clogged conditions," *Urban Water Journal*, vol. 5, no. 2, pp. 117–124, 2008.

[10] N. A. Hassan, N. A. M. Abdullah, N. A. M. Shukry et al., "Laboratory evaluation on the effect of clogging on permeability of porous asphalt mixtures," *Journal Teknologi*, vol. 76, pp. 77–84, 2015.

[11] M. Kamali, M. Delkash, and M. Tajrishy, "Evaluation of permeable pavement responses to urban surface runoff," *Journal of Environmental Management*, vol. 187, pp. 43–53, 2017.

[12] V. Andrés-Valeri, M. Marchioni, L. Sañudo-Fontaneda, F. Giustozzi, and G. Becciu, "Laboratory assessment of the infiltration capacity reduction in clogged porous mixture surfaces," *Sustainability*, vol. 8, no. 8, p. 751, 2016.

[13] M. B. Chopra, E. S. Wanielista, and M. P. Wanielista, "Pervious pavement systems in Florida-research results,," in *Proceedings of the 2010 International Low Impact Development Conference-Redefining Water in the City*, pp. 193–206, Reston, VA, USA, June 2010.

[14] R. J. Winston, A. M. Al-Rubaei, G. T. Blecken, M. Viklander, and W. F. Hunt, "Maintenance measures for preservation and recovery of permeable pavement surface infiltration rate-the effects of street sweeping, vacuum cleaning, high pressure washing, and milling," *Journal of Environmental Management*, vol. 169, no. 2, pp. 132–144, 2016.

[15] C. J. Pratt, J. D. G. Mantle, and P. A. Schofield, "UK research into the performance of permeable pavement, reservoir structures in controlling stormwater discharge quantity and quality," *Water Science and Technology*, vol. 32, no. 1, pp. 63–69, 1995.

[16] J.-D. Baladès, M. Legret, and H. Madiec, "Permeable pavements: pollution management tools," *Water Science and Technology*, vol. 32, no. 1, pp. 49–56, 1995.

[17] M. Kayhanian, D. Anderson, J. T. Harvey, D. Jones, and B. Muhunthan, "Permeability measurement and scan imaging to assess clogging of pervious concrete pavements in parking lots," *Journal of Environmental Management*, vol. 95, no. 1, pp. 114–123, 2012.

[18] N. Siriwardene, A. Deletic, and T. Fletcher, "Clogging of stormwater gravel infiltration systems and filters: insights from a laboratory study," *Water Research*, vol. 41, no. 7, pp. 1433–1440, 2007.

[19] A. Kia, H. S. Wong, and C. R. Cheeseman, "Clogging in permeable concrete: a review," *Journal of Environmental Management*, vol. 193, pp. 221–233, 2017.

[20] M. Razzaghmanesh and S. Beecham, "A review of permeable pavement clogging investigations and recommended maintenance regimes," *Water*, vol. 10, no. 337, pp. 1–9, 2018.

[21] A. M. Al-Rubaei, A. L. Stenglein, M. Viklander, and G.-T. Blecken, "Long-term hydraulic performance of porous asphalt pavements in Northern Sweden," *Journal of Irrigation and Drainage Engineering*, vol. 139, no. 6, pp. 499–505, 2013.

[22] H. P. Duncan, "An overview of urban stormwater quality," in *Proceedings of The 24th Hydrology and Water Resources Symposium*, Auckland, New Zealand, November 1997.

[23] X. J. Zuo, D. F. Fu, and H. Li, "Distribution characteristics of particle size and pollutants in road runoff during different types of rainfall," *Journal of Southeast University (Natural Science Edition)*, vol. 41, no. 2, pp. 411–415, 2011.

[24] E. S. H. Garcia, L. P. Thives, E. Ghisi, and L. N. Antunes, "Analysis of permeability reduction in drainage asphalt mixtures due to decrease in void volume," *Journal of Cleaner Production*, vol. 248, no. 1, 119292 pages, 2020.

[25] X. Cui, J. Zhang, D. Huang, W. Tang, L. Wang, and F. Hou, "Experimental simulation of rapid clogging process of pervious concrete pavement caused by storm water runoff," *International Journal of Pavement Engineering*, vol. 20, no. 1, pp. 24–32, 2019.

[26] N. Hu, J. Zhang, S. Xia et al., "A field performance evaluation of the periodic maintenance for pervious concrete pavement," *Journal of Cleaner Production*, vol. 263121463 pages, 2020.

[27] I. Bariši´c, I. N. Grubeša, T. Dokšanovi´c, and M. Zvonari´, "Influence of clogging and unbound base layer properties on pervious concrete drainage characteristics," *Materials*, vol. 13, no. 11, p. 2455, 2020.
[28] L. Chu and T. F. Fwa, "Laboratory characterization of clogging potential of porous asphalt mixtures," *Transportation Research Record: Journal of the Transportation Research Board*, vol. 2672, no. 52, pp. 12–22, 2018.
[29] S. Beecham, J. Kandasamy, and D. Pezzaniti, "Influence of clogging on the effective life of permeable pavements," *Proceedings of The Institution of Civil Engineers-Water Management*, vol. 162, no. 3, pp. 211–220, 2009.
[30] J. Sansalone, X. Kuang, and V. Ranieri, "Permeable pavement as a hydraulic and filtration interface for urban drainage," *Journal of Irrigation and Drainage Engineering*, vol. 134, no. 5, pp. 666–674, 2008.
[31] C. J. Pratt, "Permeable pavements for storm water quality enhancement in urban storm water quality enhancement: source control, retrofitting and combined sewer technology," *ASCE*, vol. 35, pp. 131–155, 1990.
[32] M. Brugin, M. Marchioni, G. Becciu, F. Giustozzi, E. Toraldo, and V. C. Andrés-Valeri, "Clogging potential evaluation of porous mixture surfaces used in permeable pavement systems," *European Journal of Environmental and Civil Engineering*, vol. 24, no. 5, pp. 620–630, 2020.
[33] A. Kia, H. S. Wong, and C. R. Cheeseman, "Defining clogging potential for permeable concrete," *Journal of Environmental Management*, vol. 220, pp. 44–53, 2018.
[34] E. Z. Bean, W. F. Hunt, and D. A. Bidelspach, "Field survey of permeable pavement surface infiltration rates," *Journal of Irrigation and Drainage Engineering*, vol. 133, no. 3, pp. 249–255, 2007.
[35] X. Ye, R. Cui, X. Du et al., "Mechanism of suspended kaolinite particle clogging in porous media during managed aquifer recharge," *Groundwater*, vol. 57, no. 5, pp. 764–771, 2019.
[36] O. Deo, M. Sumanasooriya, and N. Neithalath, "Permeability reduction in pervious concretes due to clogging: experiments and modeling," *Journal of Materials in Civil Engineering*, vol. 22, no. 7, pp. 741–751, 2010.
[37] X. Cui, J. Zhang, D. H. Chen et al., "Clogging of pervious concrete pile caused by soil piping: an approximate experimental study," *Canadian Geotechnical Journal*, vol. 55, no. 7, pp. 999–1015, 2008.
[38] H. Zhou, H. Li, A. Abdelhady, X. Liang, H. Wang, and B. Yang, "Experimental investigation on the effect of pore characteristics on clogging risk of pervious concrete based on CT scanning," *Construction and Building Materials*, vol. 212, pp. 130–139, 2019.
[39] J. Zhang, G. Ma, Z. Dai, R. Ming, X. Cui, and R. She, "Numerical study on pore clogging mechanism in pervious pavements," *Journal of Hydrology*, vol. 565, pp. 589–598, 2018.
[40] Z. Lin, H. Yang, and H. Chen, "Influence of fillers on the removal of rainwater runoff pollutants by a permeable brick system with a frame structure base," *Water Science and Technology*, vol. 80, no. 11, pp. 2131–2140, 2019.
[41] K. D. Hill and S. Beecham, "The effect of particle size on sediment accumulation in permeable pavements," *Water*, vol. 10, no. 403, pp. 1–9, 2018.
[42] X. Cui, J. Zhang, D. Chen et al., "Clogging of pervious concrete pile caused by soil piping: an approximate experimental study," *Canadian Geotechnical Journal*, vol. 212, pp. 130–139, 2017.